

Title: Modeling the impact of human mobility and travel restrictions on the potential spread of SARS-CoV-2 in Taiwan

Authors: Meng-Chun Chang^{1*}, Rebecca Kahn^{2*}, Yu-An Li¹, Cheng-Sheng Lee³, Caroline O. Buckee², Hsiao-Han Chang^{1**}

* shared first authorship

** corresponding author: hhchang@life.nthu.edu.tw

¹ Department of Life Science & Institute of Bioinformatics and Structural Biology, National Tsing Hua University, Hsinchu, Taiwan

² Department of Epidemiology & the Center for Communicable Disease Dynamics, Harvard T.H. Chan School of Public Health, Boston, MA, USA.

³ Department of Life Science & Institute of Molecular and Cellular Biology, National Tsing Hua University, Hsinchu, Taiwan

ABSTRACT

Background

As COVID-19 continues to spread around the world, understanding how patterns of human mobility and connectivity affect outbreak dynamics, especially before outbreaks establish locally, is critical for informing response efforts.

Methods

Here, in collaboration with Facebook Data for Good, we built metapopulation models that incorporate human movement data with the goals of identifying the high risk areas of disease spread and assessing the potential effects of local travel restrictions in Taiwan. We compared the impact of intracity vs. intercity travel restrictions on both the total number of infections and the speed of outbreak spread and developed an interactive application that allows users to vary inputs and assumptions.

Findings

We found that intracity travel reductions have a higher impact on overall infection numbers than intercity travel reductions, while intercity travel reductions can narrow the scope of the outbreak and help target resources. We also identified the most highly connected areas that may serve as sources of importation during an outbreak. The timing, duration, and level of travel reduction together determine the impact of travel reductions on the number of infections, and multiple combinations of these can result in similar impact.

Interpretation

In Taiwan, most cases to date were imported or linked to imported cases. To prepare for the potential spread within Taiwan, we utilized Facebook's aggregated and anonymized movement and colocation data to identify cities with higher risk of infection and regional importation. Both intracity and intercity movement affect outbreak dynamics, with the former having more of an impact on the total numbers of cases and the latter impacting geographic scope. These

findings have important implications for guiding future policies for travel restrictions during outbreaks in Taiwan.

Funding

Ministry of Science and Technology in Taiwan and National Institute of General Medical Sciences in USA

INTRODUCTION

The Coronavirus Disease 2019 (COVID-19) was first reported in Wuhan, China in December 2019 and has since caused a global pandemic, with over 500,000 confirmed cases and over 23,000 deaths reported by March 27, 2020.¹ Scientific discoveries have advanced at an unprecedented pace, with numerous clinical trials of drugs underway,² and a phase 1 vaccine trial beginning in Seattle.³ Despite these advances, no pharmaceutical interventions are yet available. In the meantime, public health officials must rely on other interventions, such as social distancing and travel restrictions, to slow the spread and reduce the peak of the outbreak, in order to prevent health systems from being overwhelmed.^{4,5}

In January 2020, as the epidemic in Wuhan grew, many countries implemented travel bans, and airlines canceled flights to attempt to slow the spread.⁶ A number of studies have estimated the risk of importation globally, with some suggesting up to two-thirds of all imported cases went undetected.^{7,8} For Taiwan, there have been 267 reported cases as of March 27, 2020⁹, with 227 imported (85%) and 40 local cases (15%). 37 local cases (92.5 %) were linked to imported or known cases, and 3 local cases (7.5 %) have unknown origin.

As the number of cases globally due to community transmission grows relative to the number of imported cases, attention has turned to more local measures to decrease spread, such as cancellations of mass gatherings, business closures, and local travel restrictions.¹⁰ Mobility data can provide critical information for responding to outbreaks and understanding the impact of travel restrictions.¹¹ Recent studies have analyzed the effects of human mobility and travel restrictions on disease spread in China.^{12,13} Here, to prepare for COVID-19 and its impact, in collaboration with Facebook Data for Good, we describe the metapopulation models we've built that include human movement data to better understand the high risk areas of disease spread and assess the potential impact of local travel restrictions in Taiwan.

METHODS

Movement data

We incorporated two different sources of movement data from Facebook into our models. In the first model, we used Facebook's newly developed colocation matrices (Facebook colocation data), which give the probability that people from two different geographic units will be in the same 600 m × 600 m location for five minutes using data over the course of a week. In the second model, we used Facebook's regular movement data (*Facebook movement data*), which

aggregates the number of trips Facebook users make between locations over time (Figure S1).¹⁴ Facebook movement data between January 26th and March 9th were used and were disaggregated by Lunar New Year (January 26th to January 29th), weekdays (Monday to Friday between January 30th and March 9th, except February 28th, a National Public Holiday in Taiwan), and weekends (Saturdays and Sundays between January 30th and March 9th plus February 28th).

Colocation covered five different weeks, with one including the Lunar New Year (January 10th to 16th) and the other four including only regular days (February 16th to 22th, February 26th to March 3rd, March 4th to March 10th, and March 11th to March 17th). As the colocation data from the four regular weeks were very similar, we used data from February 16th to 22th for our model. The geographic unit used in this study was at the centrally-governed level of “city” (here “city” indicates city, county or special municipality in Taiwan). Shape files were downloaded from Government open data platform (<https://data.gov.tw/dataset/7442>). We excluded three cities outside of the main island of Taiwan from the analysis due to their low connectivity with the main island, leaving 19 cities.

Models

We developed susceptible-exposed-infectious-recovered (SEIR) models of the spread of COVID-19 throughout Taiwan. Note that this model does not attempt to fit epidemiological dynamics to data on COVID-19 cases, and we do not account for the many complexities associated with asymptomatic transmission and different clinical outcomes. Rather, we aim to examine the spatial dynamics that would result from transmission of SARS-COV-2 across Taiwan under various mobility scenarios. As such, these dynamics may be generalizable to other pathogens with similar transmission routes.

We ran a deterministic SEIR model to analyze the overall infection dynamics, including time to peak and peak size, and we also ran the models stochastically to better understand the initial stages of disease spread. We ran the stochastic model until (1) it reached n accumulated infections or (2) the total number of infections became 0 to estimate the probability of having more than n infections (denoted by $P_{n,k}$, where k represents the number of initial infections), the time it takes to reach n infections (denoted by $T_{n,k}$), and the standard deviation of infection numbers at $T_{n,k}$ (denoted by $V_{n,k}$). To assess the initial stages of the outbreak, we used $n=1000$ and $k=3$ as our baseline values.

Let S_i , E_i , I_i , R_i be the number of susceptible, exposed, infectious, and recovered individuals in location i , respectively, and N_i be the total population in location i . Let $R_0 (=2.5)$ ¹⁵ be the average number of secondary infections from one infected individual, $D_E (=5)$ ¹⁶ be the incubation period (i.e. time from exposure to symptom onset), and $D_I (=7)$ ¹⁷ be the duration of infectiousness.

We incorporated the Facebook data into these models in two ways. In the “contact model”, we used the Facebook colocation data (C_{ij} , the probability that a person from location i collocates with a person from location j) and assumed that the contact rate between a random pair of people was proportional to C_{ij} . We scaled R_0 by $C_{ij} * N_j$ (for j not equal to i) or $C_{ii} * (N_i - 1)$, standardized to $C_{ii} * (N_i - 1)$ in Taipei, which was assumed to be the same as Wuhan.

$$\begin{aligned}\frac{dS_i}{dt} &= - \sum_{j \text{ include } i} S_i \frac{I_j}{N_j} \frac{R_{0ij}}{D_I} \\ R_{0ij} &= R_{0 \text{ Wuhan}} \frac{C_{ij} N_j}{C_{\text{Taipei-Taipei}} (N_{\text{Taipei}} - 1)} \\ R_{0ii} &= R_{0 \text{ Wuhan}} \frac{C_{ii} (N_i - 1)}{C_{\text{Taipei-Taipei}} (N_{\text{Taipei}} - 1)}\end{aligned}$$

We defined R_{0ii} as intracity R_0 and $\sum_{j \neq i} R_{0ij}$ as intercity R_0 for location i . The sum of intracity R_0 and intercity R_0 reflects total risk of infection and was standardized to the highest sum of intracity R_0 and intercity R_0 as follows:

$$\text{Risk of infection for location } i = \sum_{j \text{ include } i} R_{0ij} / \max_l (\sum_{j \text{ include } l} R_{0lj}).$$

Facebook colocation data from regular days were used to calculate risk of infection.

In the “residence model”, we first estimated the proportion of time people living in location i spend in location j (P_{ij}) based on Facebook movement data (see details in Supplementary Methods), and modeled the transmission dynamics by considering both that (1) non-travelers get infected by infectious visitors to their home location (the first part in the following equation) and that (2) naïve travelers get infected when they travel (the second part in the following equation).

$$\frac{dS_i}{dt} = -S_i P_{ii} \frac{R_0}{D_I} \frac{\sum_{j \text{ includes } i} I_j P_{ji}}{\sum_{j \text{ includes } i} N_j P_{ji}} - S_i \sum_{j \neq i} P_{ij} \frac{I_j}{N_j} \frac{R_0}{D_I}$$

The remaining equations are the same across the two models.

$$\begin{aligned}\frac{dE_i}{dt} &= \frac{-dS_i}{dt} - \frac{E_i}{D_E} \\ \frac{dI_i}{dt} &= \frac{E_i}{D_E} - \frac{I_i}{D_I} \\ \frac{dR_i}{dt} &= \frac{I_i}{D_I}\end{aligned}$$

$$N_i = S_i + E_i + I_i + R_i$$

We defined $(\sum_{j \neq i} \frac{m_{ji} N_j}{q_j}) / N_i$ as risk of regional importation (i.e. importation from other cities within Taiwan) for location i , where q_j represents the average number of subscribers in location j and m_{ji} represents the average number of people moving from location j to location i per unit of time in Facebook movement data. Source of importation was defined as the number of travelers from each location i and standardized to the highest value.

$$\text{Source of importation for location } i = \sum_{j \neq i} \frac{m_{ij}N_i}{q_i} / \max_l \left(\sum_{j \neq l} \frac{m_{lj}N_l}{q_l} \right).$$

Weekday movement data were used to calculate risk of regional importation and source of importation. Risk of regional importation, source of importation, and risk of infection defined above were calculated from movement data and represent different connectivity measures relevant for disease transmission.

One of the major differences between the contact model and the residence model is that the transmission rate within each city (R_0/D_i) varies with colocation matrices in the contact model, while it remains constant in the residence model. In this sense, the contact model is similar to the traditional density dependent model, where contact rates (and therefore transmission rates) vary with population density, and the residence model is similar to the frequency dependent model.¹⁸ As it is unclear which is most appropriate for COVID-19, we used both and compared the results.

Modeling travel reduction

To assess the potential effect of travel restrictions at multiple levels, we modeled either intra-city travel reductions, inter-city travel reductions, or a combination of both travel reductions (“overall reduction” in texts and figures) for 1, 2, 3, or 6 months or for the whole period of time. Travel reductions started from the beginning of the simulations or when there were 10, 20, 30, 50, or 100 accumulated infections. The proportion of reduction is denoted by G . In the contact model, intracity reduction was modeled by $R_{0ii}*(1-G)$ for all i , and intercity reduction was modeled by $R_{0ij}*(1-G)$ for all i not equal to j . In the residence model, intracity reduction was modeled by $R_0*(1-G)$ and intercity reduction was modeled by $P_{ij}*(1-G)$ for all i not equal to j and $P_{ii} + (1 - P_{ii})*G$ for all i .

RESULTS

Initial stage of transmission

At the end of March 2020, most cases in Taiwan were imported or linked to imported cases. Therefore, we explored a variety of initial conditions when estimating the probability of having more than 1000 infections (denoted by $P_{1000,k}$, where k represents the number of initial infections), varying both the number of initial infections and their locations. As expected, we found that, if we assumed that the transmission rates varied among cities (contact model), the probability of having more than 1000 infections also varied, with the cities with larger intracity and intercity R_0 (and larger risk of infection) showing larger P_{1000} (Figure 1, Figure S2 and Table S1). The top 5 cities with high risk of infection due to larger contact rates included Taipei City, New Taipei City, Kaohsiung City, Keelung City, Hsinchu City (Figure 2 and Table S2).

In simulations where 1000 infections were reached, the time it took to reach 1000 infections (denoted by $T_{1000,k}$) was also shorter for cities with larger intracity and intercity R_0 (Figure S3). Due to higher mobility surrounding the holiday season, $P_{1000,3}$ was higher (Figure 3) and $T_{1000,3}$ was lower during the Lunar New Year than regular days. Because of the high variation in

transmission rates in the contact model, the majority of infections at $T_{1000,3}$ were in cities with larger intracity R_0 no matter where the initial infections were (Figure S4).

When assuming that the transmission rates in different cities were the same (residence model), the probability of having more than 1000 infections and the time to reach 1000 infections did not vary much among cities (Figure 1, Figure S3 and Table S3). $P_{1000,3}$ during the Lunar New Year were not significantly different from regular weekends or weekdays either (Wilcoxon signed rank test, p -value= 0.57 [weekends] and 0.72 [weekdays]). The majority of infections at $T_{1000,3}$ were in cities with initial infections and the cities well-connected to them (Figure S4; and more details at https://roachchang.shinyapps.io/TW_CoV_Dynamics/). The effect of intercity connectivity, however, was reflected in the variation in infection numbers across cities at T_{1000} (denoted by V_{1000} ; Figure S5). The variation in infection numbers was lower in more connected cities as the chance of spreading the virus to other cities was higher.

In both models, well connected cities played more important roles, as they spread the virus to other cities more quickly and more widely. The top 5 cities with the highest risk of regional importation included Taipei City, Hsinchu City, Chiayi City, New Taipei City, and Hsinchu County, and the top 5 cities with the highest source values of importation were New Taipei City, Taipei City, Taoyuan City, Hsinchu City and Hsinchu County (Figure 2 and Table S2). In the contact model, these places also had higher intracity and intercity R_0 values (i.e. bigger cities are more densely populated and more well connected) (Table S2), further increasing the speed of the spread. Similarly, higher travel volume during the Lunar New Year increased the spread of the virus at the initial stage compared to regular days in both models.

The effect of travel restrictions at initial stage

We analyzed Facebook's movement data and found that intercity movement did not decrease between January 30th and March 9th in Taiwan among Facebook users (Figure S6A), suggesting that without travel restrictions imposed by the government, the public in Taiwan may not have reduced their frequency of travel voluntarily due to the awareness of SARS-CoV-2. We then examined the level to which travel restrictions could reduce the spread of SARS-CoV-2 in Taiwan at the initial stage of an outbreak. In both the contact model and the residence model, decreasing intracity movement had a much larger impact on $P_{1000,3}$ (Figure 1) and $T_{1000,3}$ (Figure S3) than decreasing intercity movement. The impact of reducing intercity travel was most evident in influencing how widespread the virus was: the infections were located in only a few cities at $T_{1000,3}$ if intercity travel was reduced (Figure S5).

We also examined the impact of different lengths of travel reductions (Figure 4). The probability of having more than 1000 infections decreased when the duration of intracity travel reduction increased in both models, while it did not change with the duration of intercity travel reduction. The results also suggest that higher levels of reduction and longer periods of reduction for intracity travel can have similar impacts. For example, a 60% intracity travel reduction for 2 months had similar outcomes as a 70% reduction for 1 month. While $P_{1000,3}$ did not change with the length of intercity travel reduction, longer intercity travel reduction led to slower progression of the outbreak (higher $T_{1000,3}$) in the contact model and more clustered infections (higher $V_{1000,3}$)

in both models (Figure S7). Furthermore, we found that the best timing for the travel reduction depended on both the duration of travel reduction and the level of reduction (Figure S8).

Overall dynamics

To assess the impact of travel on the overall dynamics, we performed deterministic simulations. Although the location of initial infections influenced the overall dynamics, with well-connected cities like Taipei City leading to higher total infection numbers and shorter time to peak than less-connected cities like Changhua County (Figure S9), the difference was minimal and therefore we only showed the results from Taipei (Figure 5 and Figure S10). Intracity travel reduction reduced the total number of infections and delayed time to peak in both the contact and residence models (Figure 5 and Figure S10), while intercity travel reduction had only minimal impact on the overall dynamics in both models. Similarly, increased intercity and intracity colocation probabilities during the Lunar New Year (Figure S6B) led to increased total number of infections and decreased time to peak in the contact model, but increasing only intercity movements during Lunar New Year in the residence model only shortened time to the peak minimally (Figure 5 and Figure S10), suggesting reducing large gatherings during holiday times is more important than reducing intercity travel.

DISCUSSION

By utilizing aggregated human movement data from Facebook, we built metapopulation models to understand the potential spread of SARS-CoV-2 in Taiwan given different initial conditions and to assess the potential impact of travel restrictions. We identified the top cities with the highest risk of infection as well as the top cities with the highest importation risk from other cities based on Facebook data and population sizes. We made a web-based interface showing the geographic distribution of infections at different time points (T_{100} , T_{500} and T_{1000}) in the initial stages of the outbreak given different locations of initial infections. This will help the public avoid high-risk areas, help public health professionals identify surveillance targets, and inform decisions on travel restrictions.

Consistent with previous findings showing that international travel bans are less effective than social distancing within the country,^{6,19} we found that intracity travel reduction has a higher impact on disease dynamics than intercity travel reduction and increasing the length of intracity travel reduction increases the impact. Intercity travel reduction, however, influences the variation in infection numbers across cities and can reduce the number of cities that have infections at the initial stage of the outbreak. While intercity travel did not decrease the probability of having high numbers of infections, containing the infections to a few cities has important public health impacts, as this means surveillance system can focus on fewer cities and control efforts can be more targeted.

Intracity travel reduction in our model is effectively the same as any measure that can reduce contact rates between individuals, such as social distancing, or transmission probability given contact, such as hand washing or wearing facemasks. These measures have been shown to be effective in reducing the transmission of respiratory viral pathogens in both modeling and empirical studies,^{20–24} and should be encouraged. Our study found that similar overall numbers

of infections can occur with various combinations of length of reductions and percent reduction in intracity travel (e.g. 60% reduction for 2 months had similar outcomes as 70% reduction for 1 month). The effectiveness of travel reductions varied depending on how early into the outbreak they started and their duration; for example, if restrictions lasted at least three months, starting them as early as possible had the greatest impact on $P_{1000,3}$, but if limited to only one month, starting them later sometimes had more of an impact and sometimes did not, depending on the context. Health officials can therefore take into consideration feasibility of different interventions, impact on society, and the capacity of the healthcare system to determine the optimal interventions and their duration.⁵

We found that the volume of intercity travel around Lunar New Year, where both intercity movements and intracity colocation rates increased, can significantly increase the speed of virus spread. Another traditional holiday, Ching Ming festival, is coming soon (April 2 to 5), and the volume of human movement between cities during this period is expected to increase like Lunar New Year, but at a lower level. Our results suggest that it is important to avoid travel or reduce the impact of travel through measures such as limiting social interactions and wearing facemasks when taking public transportation to reduce the spread of the virus.

Although we did not observe a significant change in intercity movements from January 30th to March 8th, Facebook data have the potential to track how the volume and pattern of travel change through time as the outbreak progresses, and we can incorporate any change in human mobility into the metapopulation models in nearly real time to help fight COVID-19.^{11,25} Moreover, our model utilizing human mobility data from Facebook is not limited to intercity or intracity level, or Taiwan. Facebook movement data are also calculated at finer geographic scales (such as towns) and for other countries, and our model can be easily applied in these settings to understand disease dynamics of COVID-19.

Acknowledgments

We thank Brian Karrer, Alex Pompe, Laura McGorman for their contributions.

REFERENCES

1. The World Health Organization. Coronavirus disease 2019 (COVID-19) Situation Report – 67 [Internet]. 2020. Available from: https://www.who.int/docs/default-source/coronaviruse/situation-reports/20200327-sitrep-67-covid-19.pdf?sfvrsn=b65f68eb_4
2. Maxmen A. More than 80 clinical trials launch to test coronavirus treatments. *Nature*. 2020;578(7795):347.
3. NIH. NIH clinical trial of investigational vaccine for COVID-19 begins. 2020 Mar 16; Available from: <https://www.nih.gov/news-events/news-releases/nih-clinical-trial-investigational-vaccine-covid-19-begins>
4. Ferguson NM, Laydon D, Nedjati-gilani G, Imai N, Ainslie K, Baguelin M, et al. Impact of non-pharmaceutical interventions (NPIs) to reduce COVID- 19 mortality and healthcare demand. 2020;(March).
5. Kissler SM, Tedijanto C, Lipsitch M, Grad Y. Social distancing strategies for curbing the COVID-19 epidemic. medRxiv [Internet]. 2020 Jan 1;2020.03.22.20041079. Available from: <http://medrxiv.org/content/early/2020/03/24/2020.03.22.20041079.abstract>
6. Chinazzi M, Davis JT, Ajelli M, Gioannini C, Litvinova M, Merler S, et al. The effect of travel restrictions on the spread of the 2019 novel coronavirus (COVID-19) outbreak. *Science* (80-). 2020;
7. Bhatia S, Imai N, Cuomo-dannenburg G, Baguelin M, Boonyasiri A, Cori A, et al. Report 6 : Relative sensitivity of international surveillance. 2020;(Figure 1):1–6.
8. Niehus R, De Salazar PM, Taylor A, Lipsitch M. Quantifying bias of COVID-19 prevalence and severity estimates in Wuhan, China that depend on reported cases in international travelers. medRxiv [Internet]. 2020 Jan 1;2020.02.13.20022707. Available from: <http://medrxiv.org/content/early/2020/02/18/2020.02.13.20022707.abstract>
9. Taiwan CDC. COVID-19.
10. World Health Organization. Responding to community spread of COVID-19. 2020;(March):1–6.
11. Buckee CO, Balsari S, Chan J, Crosas M, Dominici F, Gasser U, et al. Aggregated mobility data could help fight COVID-19. *Science* (80-) [Internet]. 2020 Mar 23;eabb8021. Available from: <http://science.sciencemag.org/content/early/2020/03/20/science.abb8021.abstract>
12. Li R, Pei S, Chen B, Song Y, Zhang T, Yang W, et al. Substantial undocumented infection facilitates the rapid dissemination of novel coronavirus (SARS-CoV2). *Science* (80-) [Internet]. 2020 Mar 16;eabb3221. Available from: <http://science.sciencemag.org/content/early/2020/03/13/science.abb3221.abstract>
13. Kraemer MUG, Yang C-H, Gutierrez B, Wu C-H, Klein B, Pigott DM, et al. The effect of human mobility and control measures on the COVID-19 epidemic in China. *Science* (80-) [Internet]. 2020 Mar 25;eabb4218. Available from: <http://science.sciencemag.org/content/early/2020/03/25/science.abb4218.abstract>
14. Maas P, Nayak C, Dow A, Gros A, Mason W, Filiz IO, et al. Facebook Disaster Maps: Methodology. *Faceb Res* [Internet]. 2017;1–10. Available from: <https://research.fb.com/facebook-disaster-maps-methodology/>
15. World Health Organization (WHO). Coronavirus disease 2019 (COVID-19) Situation Report – 46 [Internet]. 2020. Available from: <https://www.who.int/docs/default->

- source/coronaviruse/situation-reports/20200306-sitrep-46-covid-19.pdf?sfvrsn=96b04adf_2
16. Bi Q, Wu Y, Mei S, Ye C, Zou X, Zhang Z, et al. Epidemiology and Transmission of COVID-19 in Shenzhen China: Analysis of 391 cases and 1,286 of their close contacts. medRxiv [Internet]. 2020 Jan 1;2020.03.03.20028423. Available from: <http://medrxiv.org/content/early/2020/03/19/2020.03.03.20028423.abstract>
 17. Centers for Disease Control and Prevention. Coronavirus Disease 2019 (COVID-19) [Internet]. 2020. Available from: <https://www.cdc.gov/coronavirus/2019-ncov/if-you-are-sick/care-for-someone.html>
 18. McCallum H, Barlow N, Hone J. How should pathogen transmission be modelled? Trends Ecol Evol. 2001;16(6):295–300.
 19. Wu JT, Leung K, Leung GM. Nowcasting and forecasting the potential domestic and international spread of the 2019-nCoV outbreak originating in Wuhan, China: a modelling study. Lancet. 2020;395(10225):689–97.
 20. Lai S, Ruktanonchai NW, Zhou L, Prosper O, Luo W, Floyd JR, et al. Effect of non-pharmaceutical interventions for containing the COVID-19 outbreak in China. medRxiv [Internet]. 2020 Jan 1;2020.03.03.20029843. Available from: <http://medrxiv.org/content/early/2020/03/13/2020.03.03.20029843.abstract>
 21. Prem K, Liu Y, Russell T, Kucharski AJ, Eggo RM, Davies N, et al. The effect of control strategies that reduce social mixing on outcomes of the COVID-19 epidemic in Wuhan, China. medRxiv [Internet]. 2020 Jan 1;2020.03.09.20033050. Available from: <http://medrxiv.org/content/early/2020/03/12/2020.03.09.20033050.abstract>
 22. Anderson RM, Heesterbeek H, Klinkenberg D, Hollingsworth TD. How will country-based mitigation measures influence the course of the COVID-19 epidemic? Lancet. 2020;395(10228):931–4.
 23. Cowling BJ, Chan K-H, Fang VJ, Cheng CKY, Fung ROP, Wai W, et al. Facemasks and hand hygiene to prevent influenza transmission in households: a cluster randomized trial. Ann Intern Med. 2009;151(7):437–46.
 24. Tracht SM, Del Valle SY, Hyman JM. Mathematical Modeling of the Effectiveness of Facemasks in Reducing the Spread of Novel Influenza A (H1N1). PLoS One [Internet]. 2010 Feb 10;5(2):e9018. Available from: <https://doi.org/10.1371/journal.pone.0009018>
 25. Emanuele Pepe, Paolo Bajardi, Laetitia Gauvin, Filippo Privitera, Ciro Cattuto MT. COVID-19 outbreak response: first assessment of mobility changes in Italy following lockdown [Internet]. 2020. Available from: <https://covid19mm.github.io/in-progress/2020/03/13/first-report-assessment.html>

FIGURES

Figure 1. The probability of having 1000 infections. $P_{1000,3}$ from simulations with initial infections in Taipei City (representing big cities) or Changhua County (representing small cities) using both contact and residence models are shown. The difference between big and small cities was more significant in the contact model than in the residence model. Intracity and intercity travel reduction reduced $P_{1000,3}$, while the impact of intercity travel reduction was minor. Increased human mobility during Lunar New Year increased $P_{1000,3}$.

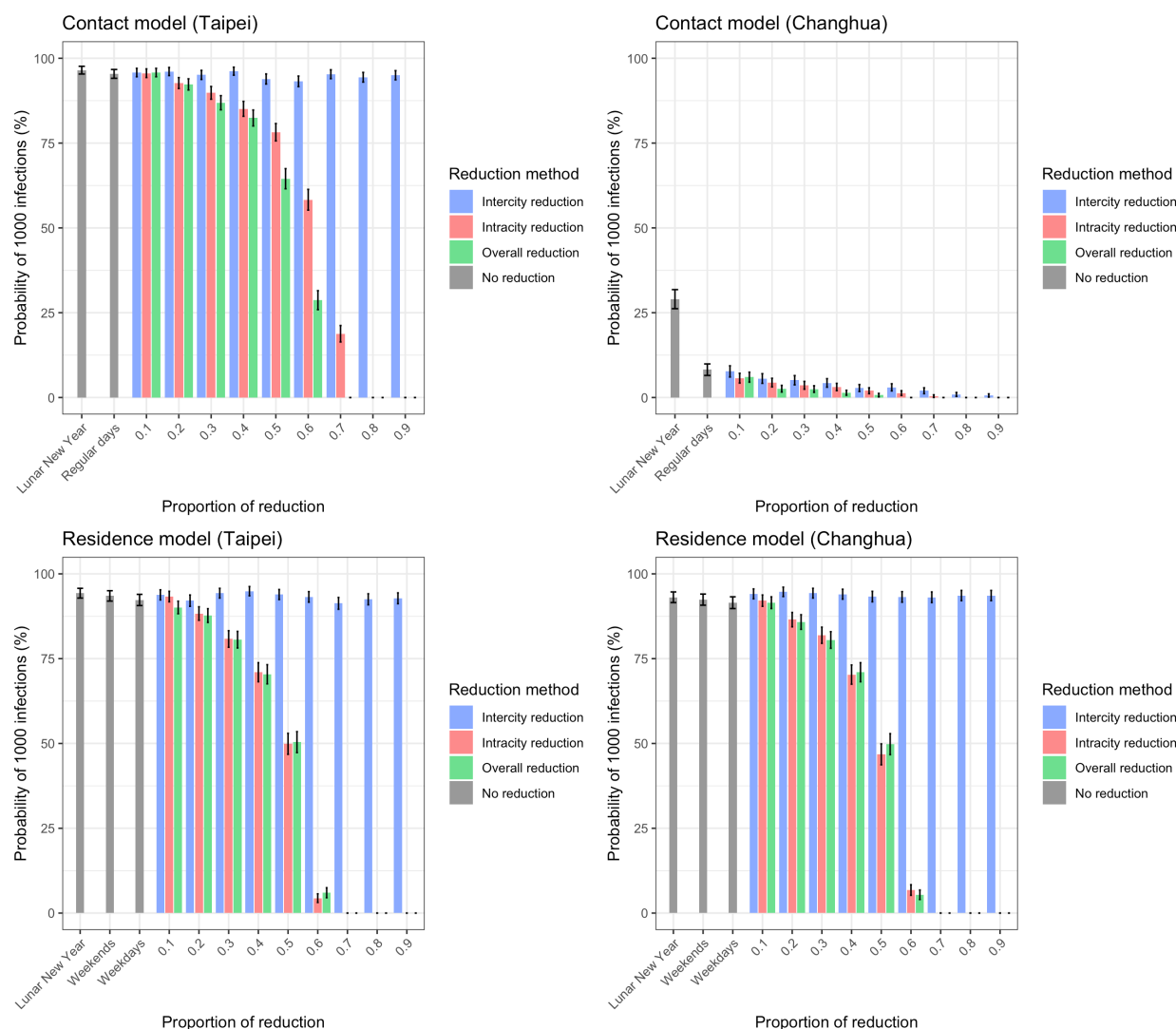


Figure 2. Connectivity measures. Three kinds of connectivity measures relevant to disease spread are shown. The values for bigger cities were larger. (A) Risk of infection. (B) Risk of importation. (C) Source of importation.

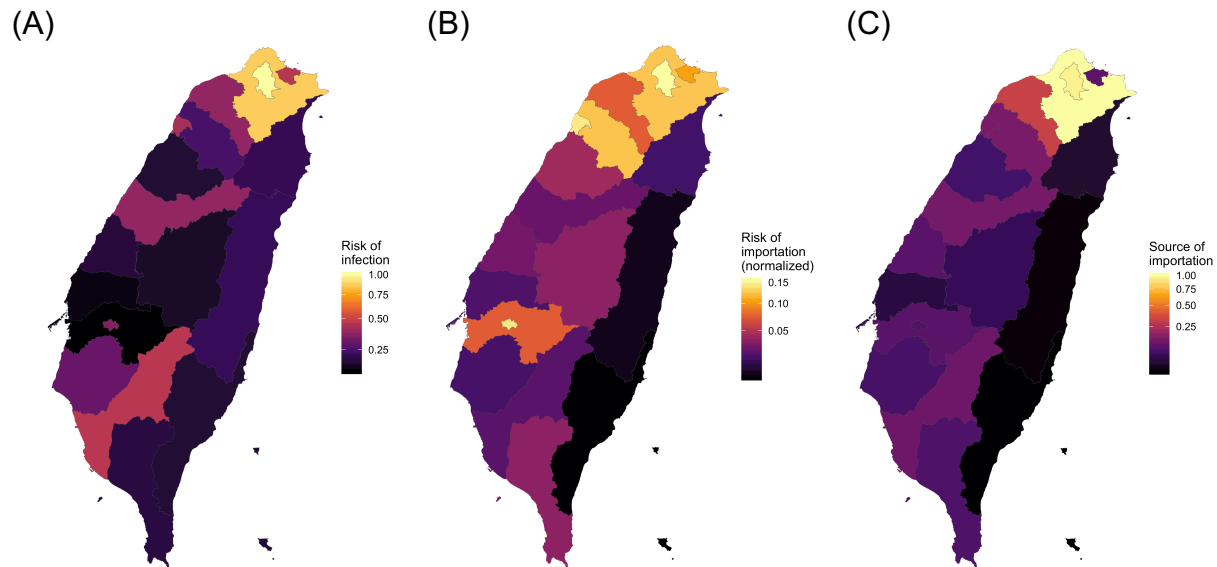


Figure 3. The probability of having 1000 infections was higher with human movements during Lunar New year. $P_{1000,3}$ was significantly higher if human mobility during Lunar New Year was used (Wilcoxon signed rank test, p -value= 3.82×10^{-6}). Each point represents a city in Taiwan, and the red line is the $x=y$ line.

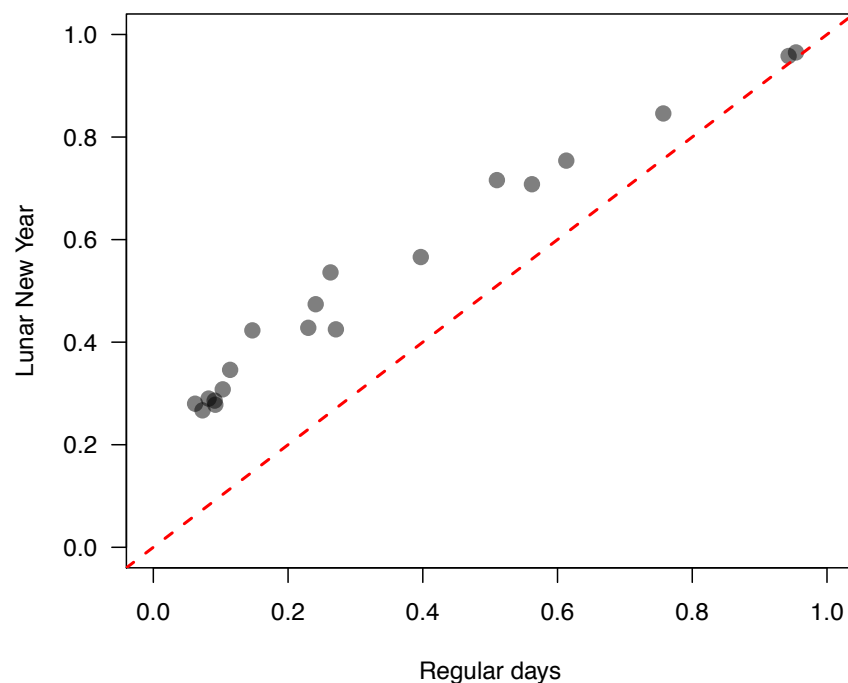


Figure 4. The impact of the duration of travel reduction and the level of reduction on the probability of having 1000 infections. $P_{1000,3}$ from the contact model (A) and the residence model (B) with initial infections in Taipei City. The color represents the level of reduction in $P_{1000,3}$ (white to red represents smaller to larger reduction). As the duration of intracity travel reduction increased, $P_{1000,3}$ decreased in both models. $P_{1000,3}$ did not change with the duration of intercity travel reduction.

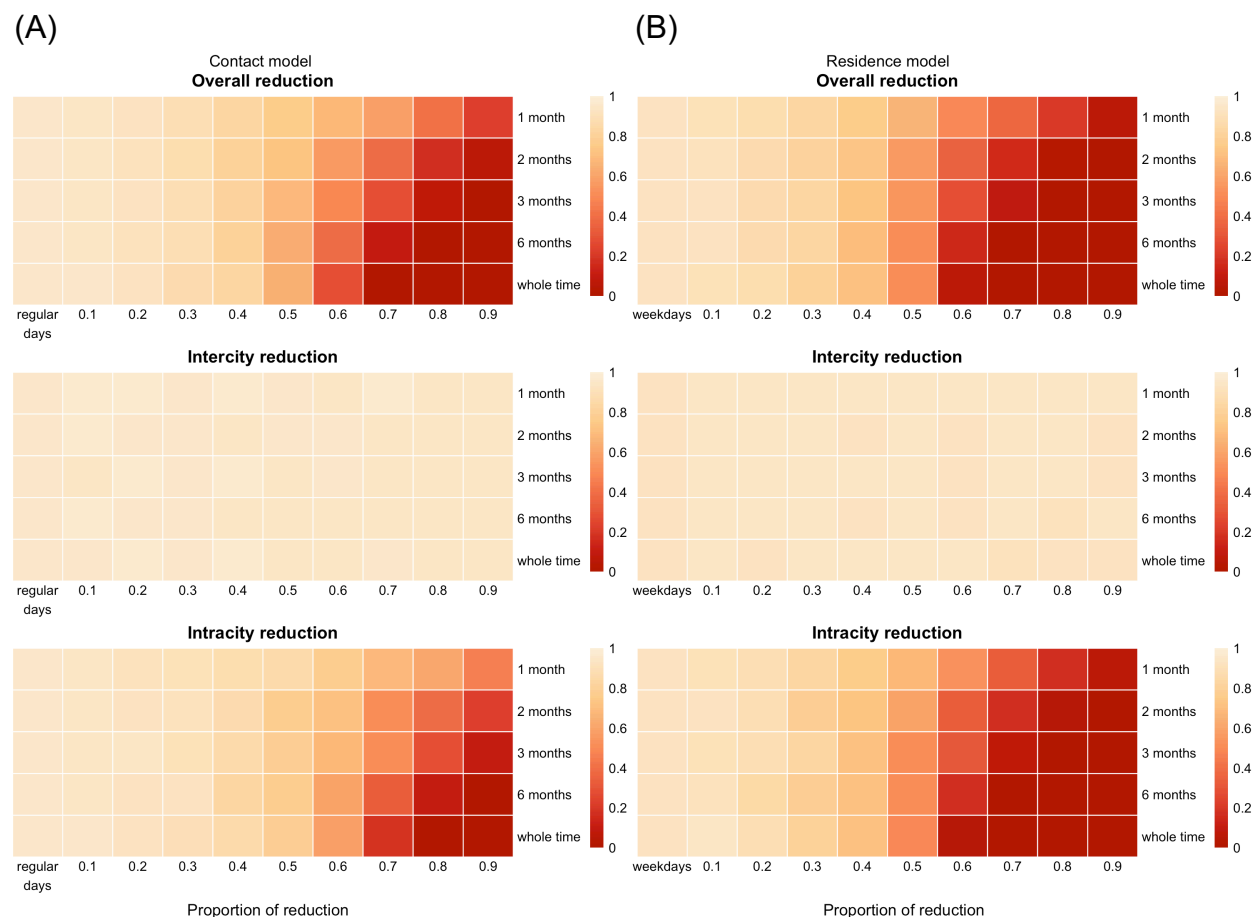
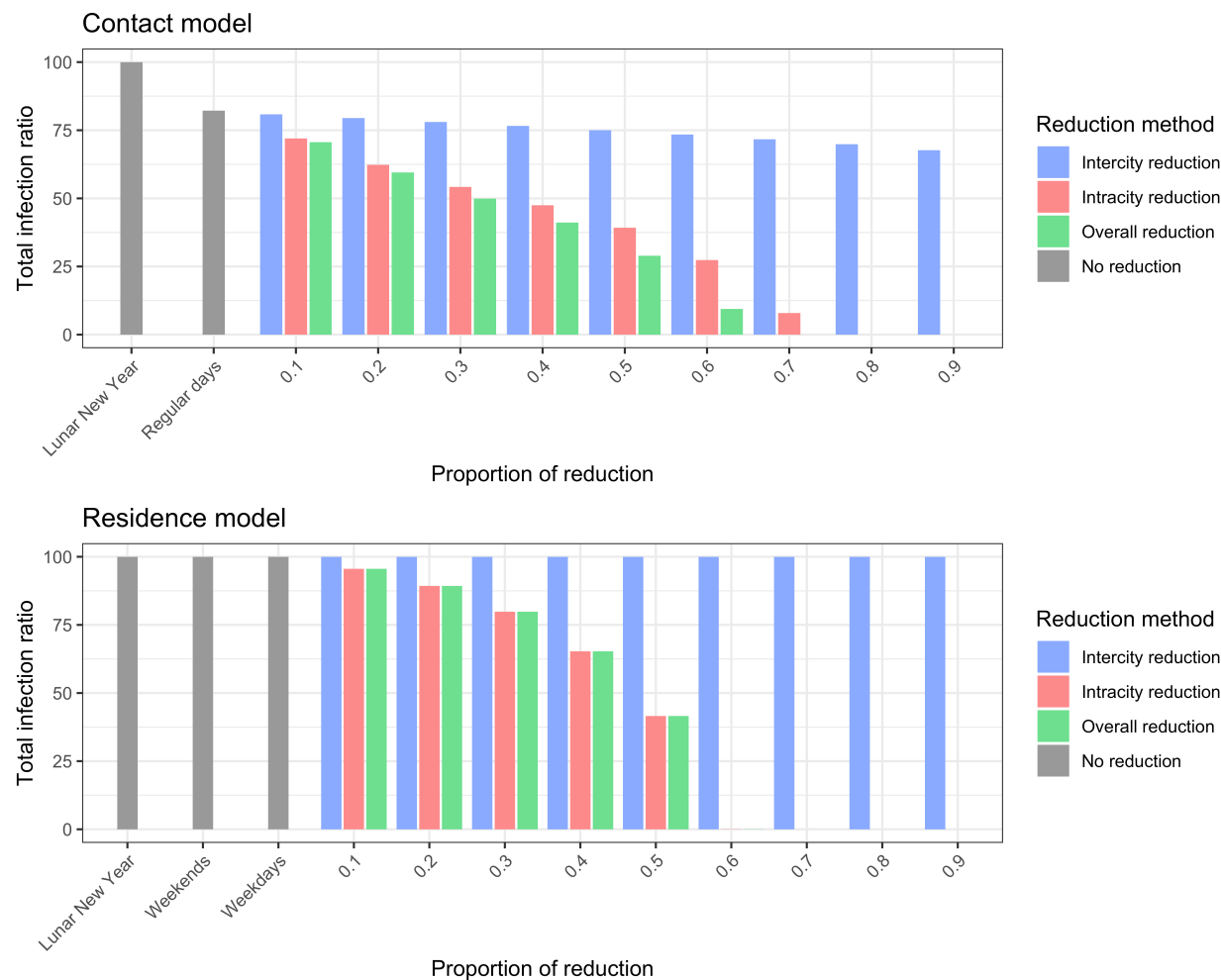


Figure 5. Reduction in total number of infections by different kinds of travel reduction.

Total infection ratio represents the ratio of total infections with travel reduction to total infections without travel reduction. The ratios shown here are from deterministic simulations with initial infections in Taipei City. Intracity and overall travel reduction effectively decreased the total number of infections. The impact of intercity travel reduction was small. For some conditions, number of infections decreased from the beginning of simulations and no bar was shown.



SUPPLEMENTARY MATERIALS

SUPPLEMENTARY METHODS

Estimating P_{ij}

We built a travel model to estimate the proportion of time people living in location i spend in location j (P_{ij}) by fitting the model to the Facebook movement data. X_{ij} represents the proportion of people living in location i currently in location j , and \widehat{X}_{ij} represents the equilibrium state of X_{ij} , and its value under the fitted model is used as our estimate of P_{ij} . People living in location i travel with probability F_i , and the probability that a traveler from location i travels to location j is denoted by T_{ij} . Travelers go back to their home location at probability λ_i per unit of time. $M_{ij,t,t+1}$ represents the number of people moving from location i to location j between time t and $t+1$.

$$\begin{aligned} X_{ij}(t+1) &= X_{ij}(t) + X_{ii}(t)F_iT_{ij} - X_{ij}(t)\lambda_i \\ X_{ii}(t+1) &= X_{ii}(t) - X_{ii}(t)F_i + \sum_{j \neq i} X_{ij}(t)\lambda_i \\ M_{ij,t,t+1} &= N_iX_{ii}(t)F_iT_{ij} + N_jX_{ji}(t)\lambda_j \\ M_{ii,t,t+1} &= N_iX_{ii}(t)(1 - F_i) + \sum_{j \neq i} N_jX_{ji}(t)(1 - \lambda_j) \end{aligned}$$

At equilibrium,

$$\widehat{X}_{ij} = \frac{F_iT_{ij}}{F_i + \lambda_i}, \widehat{X}_{ii} = \frac{\lambda_i}{F_i + \lambda_i}, \widehat{M}_{ij} = \frac{N_iF_iT_{ij}\lambda_i}{F_i + \lambda_i} + \frac{N_jF_jT_{ji}\lambda_j}{F_j + \lambda_j}, \text{ and } \widehat{M}_{ii} = \frac{N_i(1-F_i)\lambda_i}{F_i + \lambda_i} + \sum_{j \neq i} \frac{N_jF_jT_{ji}(1-\lambda_j)}{F_j + \lambda_j}.$$

For simplicity, we assumed that the majority of travel is work-related travel and on average travelers spend eight hours in the travel destination ($\lambda_i = 1$ given the unit of time is 8 hours) and that T_{ij} is proportional to M_{ij} , leaving F_i the only parameters to be fitted. We used a gradient descent algorithm to find the local optimum solution for F_i , where the cost function is defined by the sum of the squared difference between normalized m_{ij} and the normalized value of M_{ij} from the model. We calculated \widehat{X}_{ij} under fitted parameters to obtain estimates of P_{ij} .

SUPPLEMENTARY FIGURES

Figure S1. Movement patterns estimated from the Facebook data in Taiwan. (A) Regular movement data. (B) Colocation matrices.

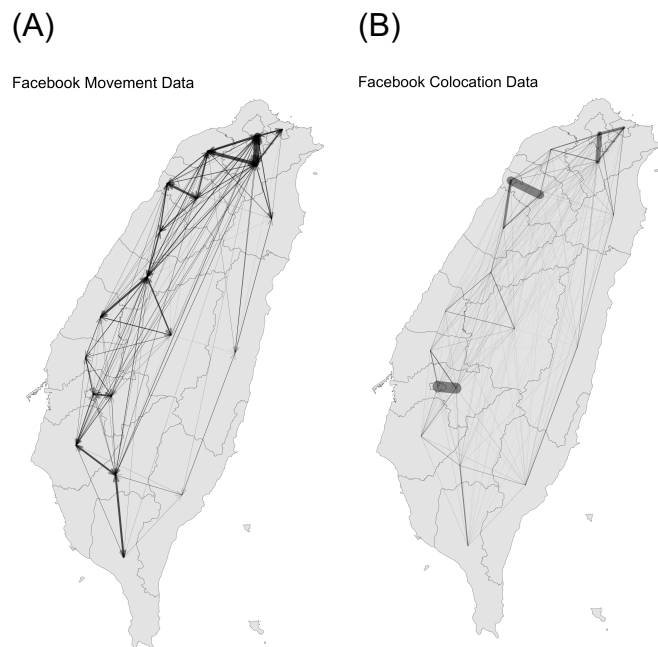


Figure S2. The probability of having a large number of infections was associated with intracity and intercity R_0 and risk of infection. Both intracity and intercity R_0 were positively correlated with $P_{1000,3}$ (Pearson's correlation test, $r=0.93$ [intracity], 0.83 [intercity], and 0.94 [risk of infection], p -value= 1.28×10^{-8} , 1.34×10^{-5} [intercity], and 4.03×10^{-9} [risk of infection]). Intercity and intracity R_0 were also positively correlated (Pearson's correlation test, $r=0.80$, p -value= 3.75×10^{-5} , not shown).

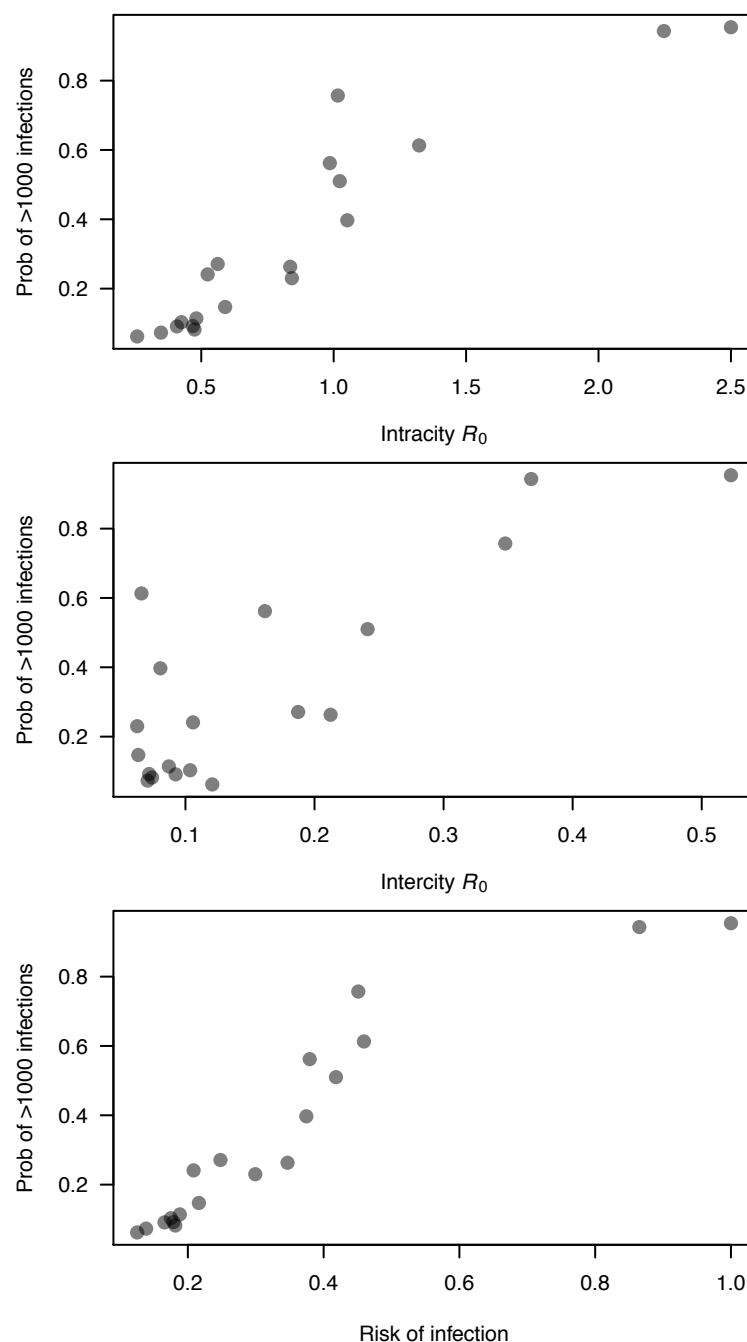


Figure S3. Time to reach 1000 accumulated infections. If initial infections were in a big city, it took less time to reach 1000 infections in the contact model. The difference between big and small cities was not significant in the residence model. Intracity and overall travel reduction delayed the time to reach 1000 infections in both models, while intercity reduction did not. For some conditions, $P_{1000,3}$ was 0 and no bar was shown.

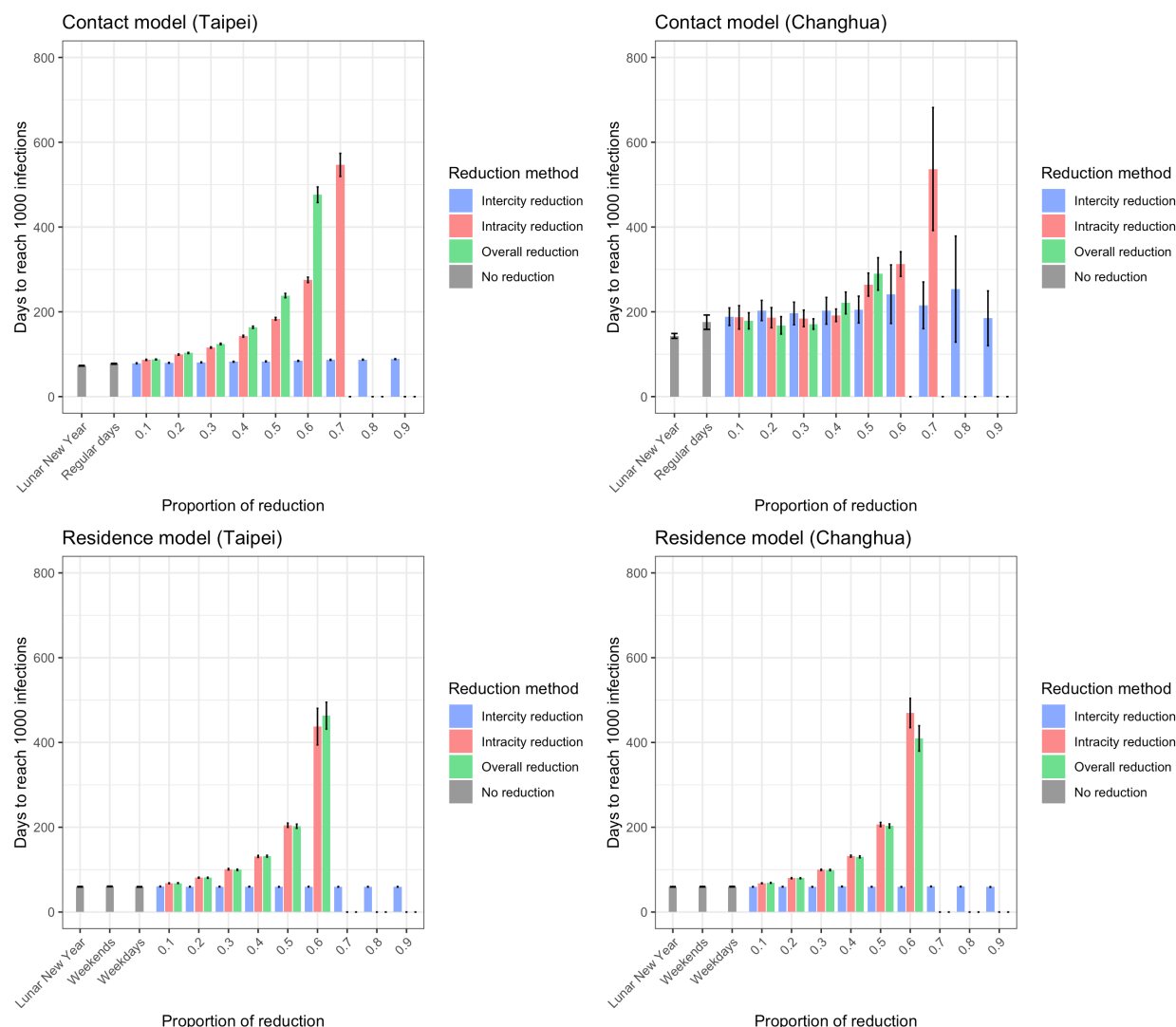


Figure S4. The distribution of infections at $T_{1000,3}$. The location of initial three infections is labeled with a white border. In the contact model, the first 1000 infections were in big cities; in the residence model, the first 1000 infections were located in cities with initial infections and the cities well-connected to them.

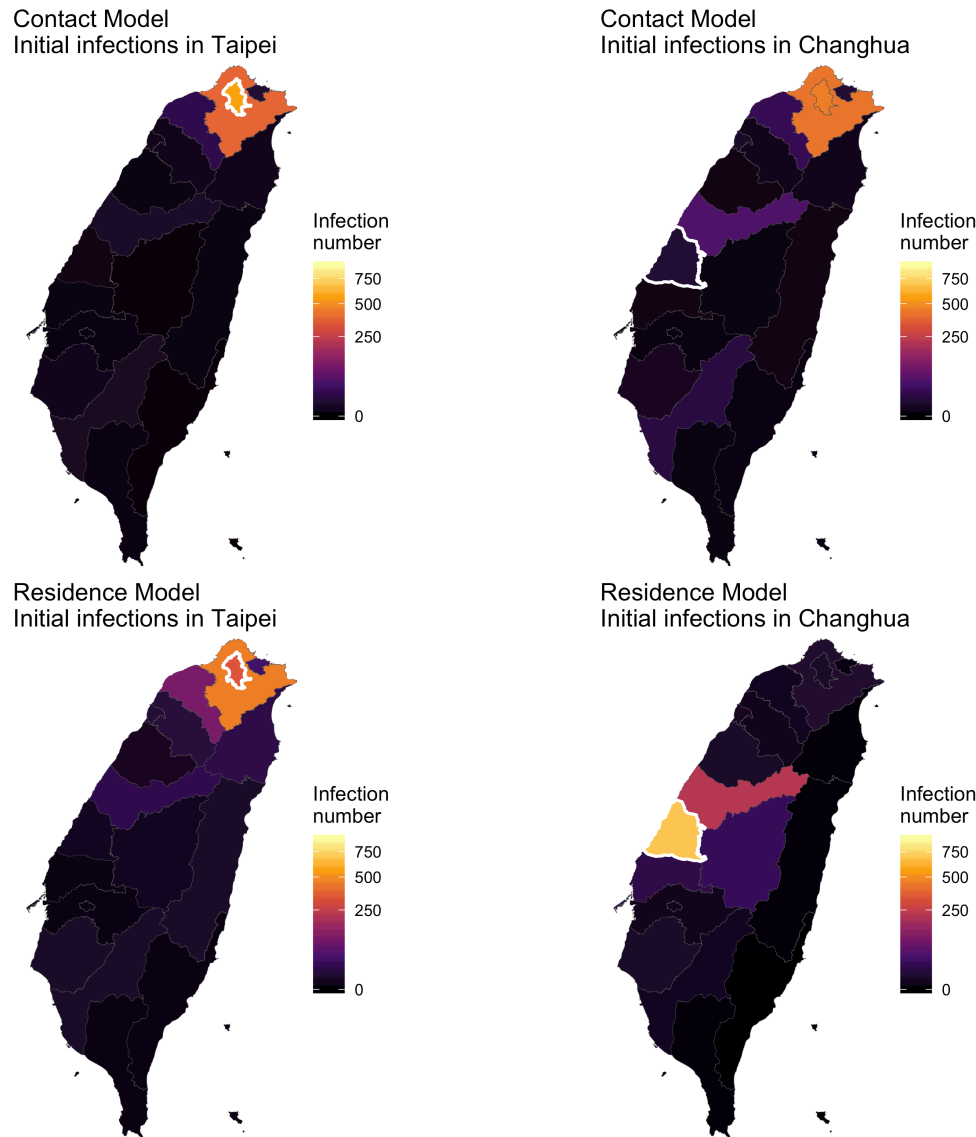


Figure S5. Standard deviation of infection numbers across different cities at $T_{1000,3}$ ($V_{1000,3}$). Intercity travel reduction increased the variation in infection numbers across cities in both models.

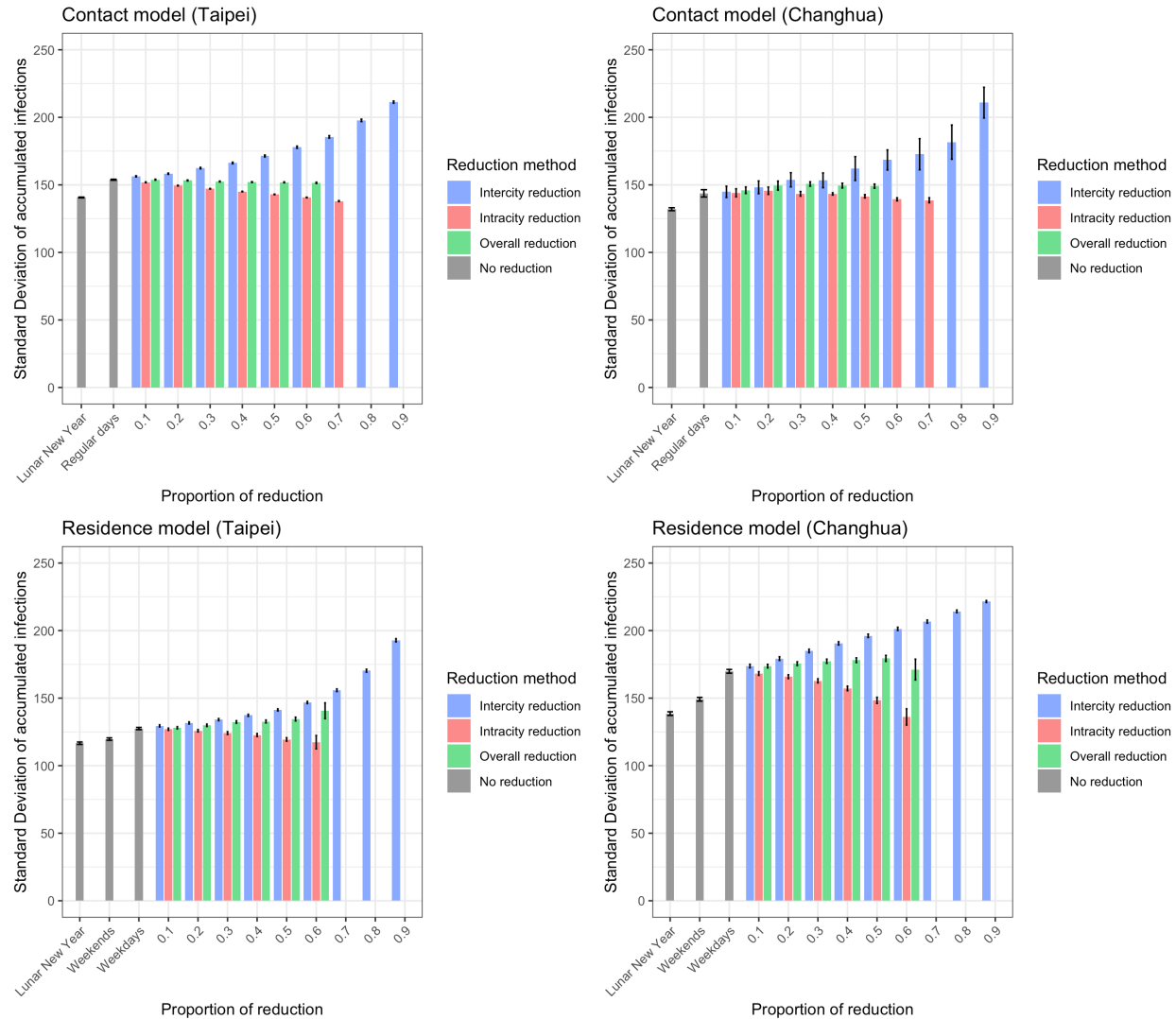


Figure S6. The frequency of travel between January 26th and March 9th. Lunar New Year ended on January 29th. The frequency of travel did not decrease after Jan 30th. Three travel routes are shown here, including a small city to big city (Changhua County to Taipei City), a big city to big city (Taipei City to New Taipei City) and a big city to small city (Taipei City to Yilan County).

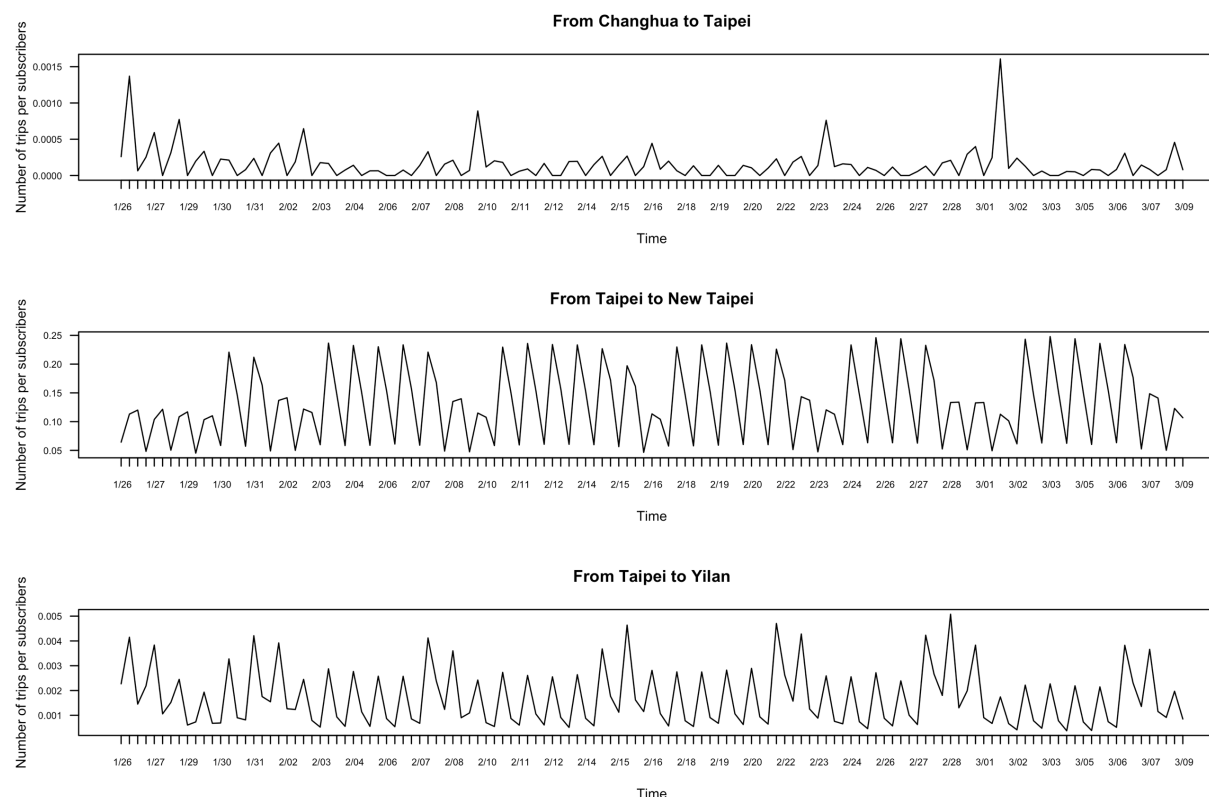


Figure S7. $T_{1000,3}$ and $V_{1000,3}$ under different lengths of intercity travel reduction. $T_{1000,3}$ (upper panel) and $V_{1000,3}$ (lower panel).

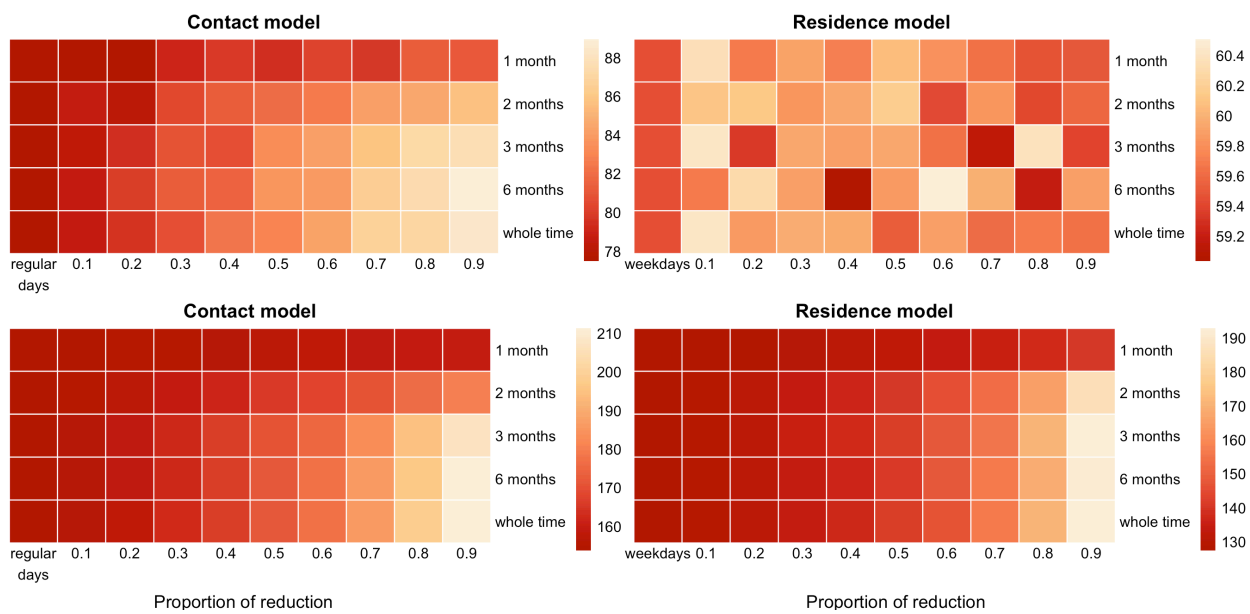
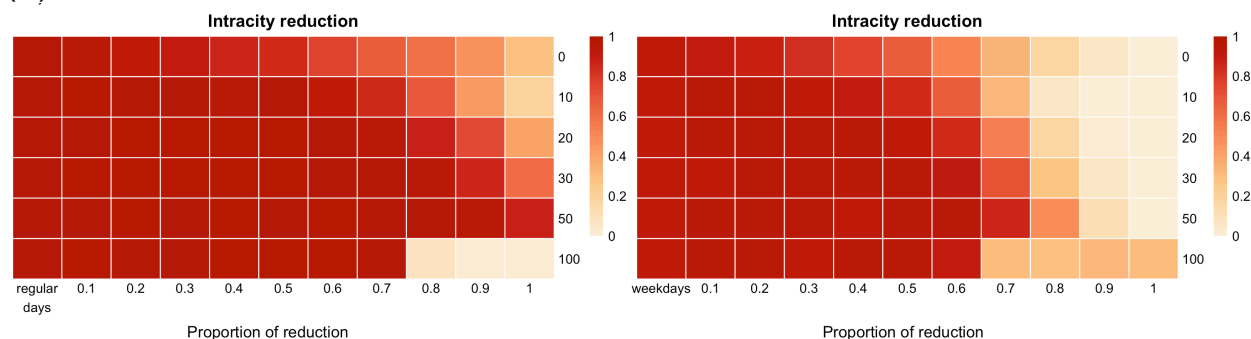


Figure S8. $P_{1000,3}$ when travel reduction started at different conditions. $P_{1000,3}$ when travel reduction started from the beginning of the simulations (denoted by 0), or when there were 10, 20, 30, 50, and 100 infections in both contact (left) and residence (right) models. Two different lengths of travel reduction duration were shown: (A) 1 month (B) 3 months. Only intracity travel reduction was shown here because intercity travel reduction only had minimal impact on $P_{1000,3}$ and the results from overall reduction and intracity reduction were qualitatively similar. The timings associated with the lowest $P_{1000,3}$ differed for one-month and three-month travel reductions. It was best to reduce travel at the beginning if the duration was for three months, but the pattern for one-month travel reduction was more complicated.

(A)



(B)

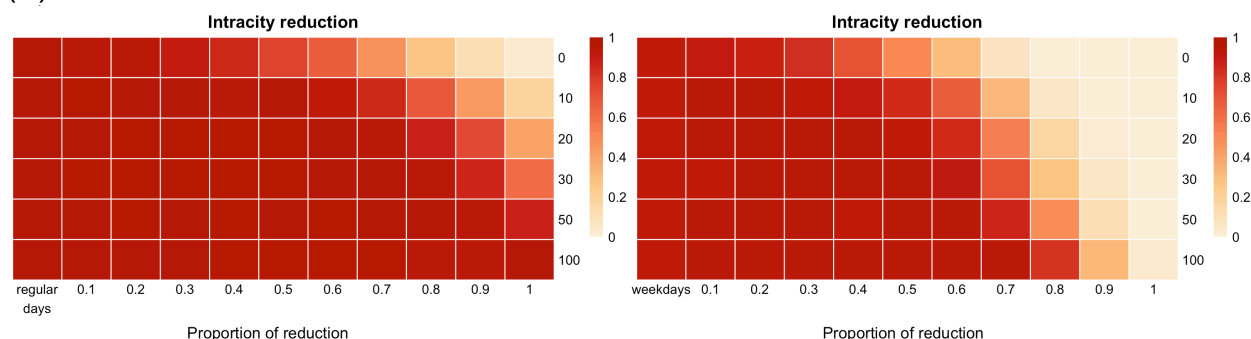


Figure S9. Comparison of overall dynamics with initial infections in big and small cities.

Total infection ratio and the ratio of time to peak are the infection numbers and the time to peak standardized to the highest values, respectively. The total infection numbers were similar between the outbreaks seeded by infections from big and small cities. The time to peak was slightly longer if the outbreak was initiated with infections in a small city.

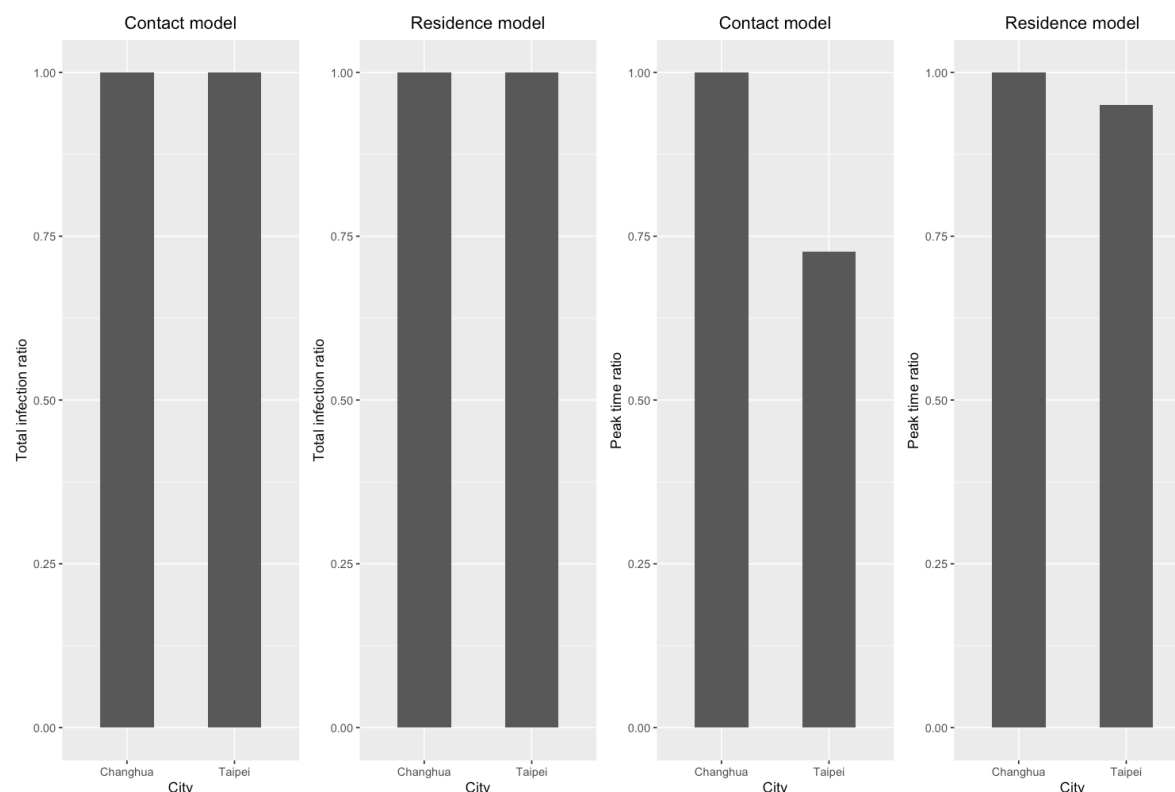
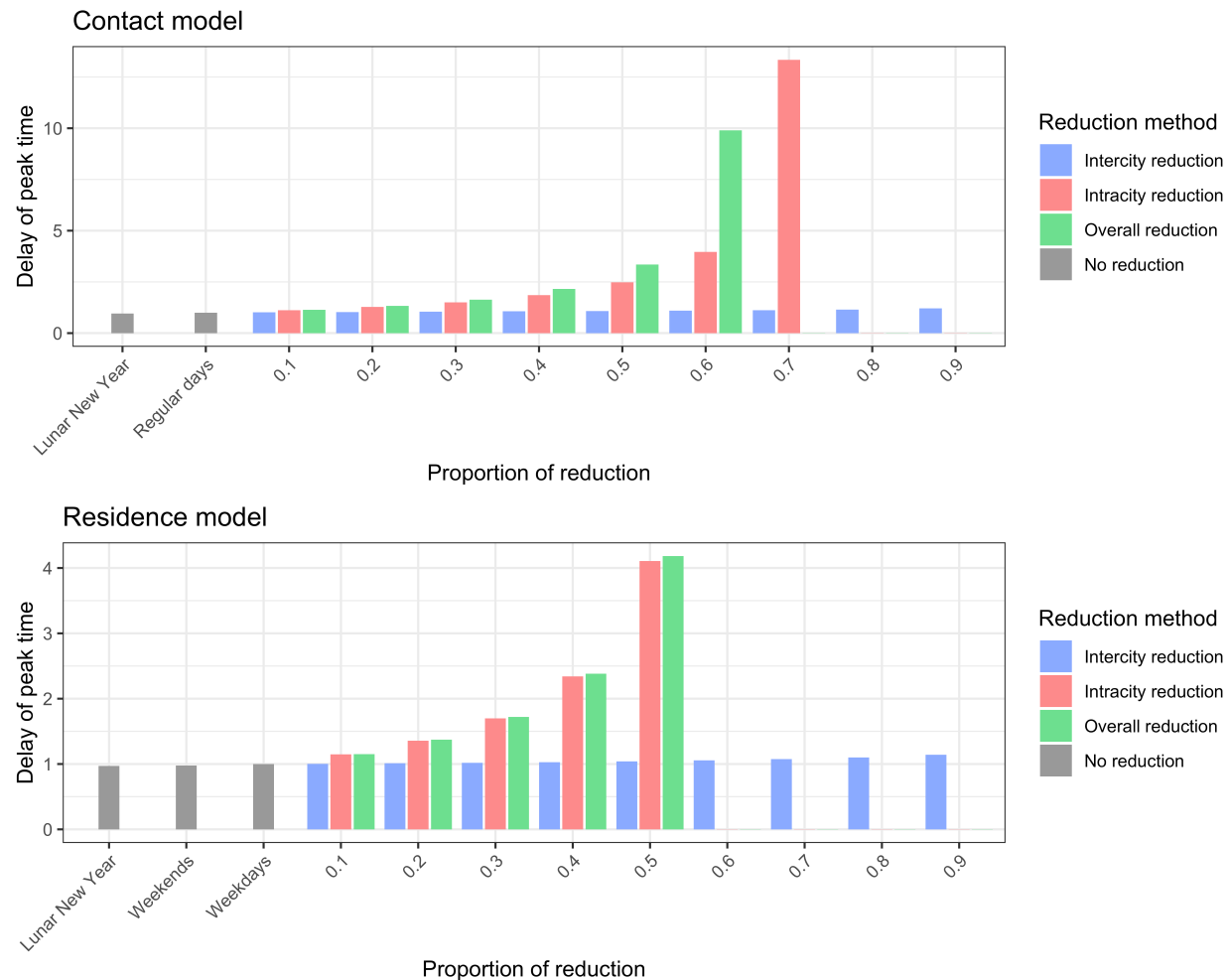


Figure S10. The delay in peak time by travel reduction. The time to peak was standardized to regular days in the contact model and to weekdays in the residence model. The time to peak increased significantly with intracity and overall travel reduction, but only increased minimally with intercity reduction.



SUPPLEMENTARY TABLES

Table S1. The probability of having 1000 infections given different numbers of initial infections in different cities (contact model). Colocation matrices in regular days were used.

	1	2	3	4	5	6	7	8	9	10
Keelung City	0.378	0.591	0.757	0.854	0.895	0.920	0.956	0.963	0.984	0.989
New Taipei City	0.608	0.857	0.943	0.976	0.991	0.997	0.997	0.999	1	1
Taipei City	0.677	0.871	0.954	0.983	0.992	0.997	1	1	1	1
Taoyuan City	0.247	0.437	0.562	0.663	0.753	0.820	0.865	0.888	0.919	0.940
Hsinchu County	0.094	0.211	0.271	0.356	0.400	0.443	0.545	0.592	0.615	0.633
Hsinchu City	0.232	0.399	0.510	0.620	0.726	0.781	0.829	0.866	0.897	0.907
Miaoli County	0.055	0.092	0.103	0.147	0.213	0.246	0.276	0.300	0.299	0.376
Taichung City	0.157	0.266	0.397	0.485	0.568	0.633	0.690	0.727	0.770	0.814
Changhua County	0.033	0.045	0.082	0.121	0.151	0.144	0.186	0.203	0.232	0.237
Yunlin County	0.021	0.048	0.073	0.099	0.109	0.141	0.155	0.185	0.195	0.216
Chiayi County	0.026	0.059	0.062	0.098	0.109	0.142	0.135	0.200	0.189	0.220
Chiayi City	0.088	0.174	0.263	0.338	0.391	0.452	0.463	0.534	0.590	0.635
Nantou County	0.031	0.047	0.091	0.097	0.130	0.171	0.182	0.197	0.215	0.240
Tainan City	0.065	0.137	0.230	0.234	0.309	0.351	0.416	0.436	0.446	0.491
Kaohsiung City	0.268	0.449	0.613	0.710	0.803	0.829	0.888	0.927	0.950	0.952
Pingtung County	0.041	0.086	0.114	0.154	0.183	0.216	0.267	0.295	0.303	0.335
Taitung County	0.028	0.069	0.092	0.137	0.160	0.202	0.231	0.246	0.291	0.313
Hualien County	0.056	0.087	0.147	0.193	0.274	0.279	0.310	0.322	0.388	0.408
Yilan County	0.103	0.170	0.241	0.334	0.369	0.478	0.489	0.527	0.561	0.619

Table S2. Intracity R_0 , intercity R_0 , risk of infection, and risk of importation.

City	Intracity R_0	Intercity R_0	Risk of infection	Risk of importation	Source of importation
Keelung City	1.016	0.348	0.451	0.107	0.095
New Taipei City	2.247[#]	0.368	0.865	0.125	1.000
Taipei City	2.500	0.523	1.000	0.155	0.951
Taoyuan City	0.985	0.162	0.379	0.073	0.321
Hsinchu County	0.562	0.187	0.248	0.123	0.136
Hsinchu City	1.023	0.241	0.418	0.143	0.138
Miaoli County	0.425	0.104	0.175	0.044	0.062
Taichung City	1.051	0.081	0.375	0.026	0.130
Changhua County	0.475	0.074	0.182	0.029	0.089
Yunlin County	0.348	0.071	0.138	0.019	0.031
Chiayi County	0.258	0.121	0.125	0.073	0.084
Chiayi City	0.836	0.212	0.347	0.141	0.075

Nantou County	0.408	0.092	0.166	0.036	0.047
Tainan City	0.842	0.063	0.299	0.019	0.069
Kaohsiung City	1.323	0.066	0.459	0.022	0.124
Pingtung County	0.482	0.087	0.188	0.036	0.071
Taitung County	0.468	0.072	0.179	0.004	0.003
Hualien County	0.590	0.063	0.216	0.006	0.005
Yilan County	0.524	0.106	0.208	0.018	0.019

#Top five values in each column are bold.

Table S3. The probability of having 1000 infections given different numbers of initial infections in different cities (residence model). Movement data on weekdays were used.

	1	2	3	4	5	6	7	8	9	10
Keelung City	0.595	0.857	0.941	0.970	0.993	0.998	0.999	1	1	1
New Taipei City	0.585	0.832	0.945	0.965	0.984	0.993	0.998	0.999	0.998	1
Taipei City	0.613	0.847	0.923	0.973	0.992	0.994	0.996	0.999	0.999	1
Taoyuan City	0.603	0.819	0.935	0.978	0.991	0.998	0.999	1	1	1
Hsinchu County	0.584	0.842	0.948	0.982	0.991	0.997	0.997	1	1	1
Hsinchu City	0.594	0.849	0.927	0.975	0.990	0.994	1	0.999	1	1
Miaoli County	0.567	0.853	0.931	0.978	0.987	0.997	0.999	1	1	1
Taichung City	0.584	0.837	0.953	0.972	0.989	0.994	0.997	0.999	0.999	1
Changhua County	0.586	0.838	0.915	0.970	0.994	0.996	0.996	0.999	1	1
Yunlin County	0.589	0.826	0.926	0.981	0.993	0.997	1	0.999	1	1
Chiayi County	0.598	0.828	0.945	0.972	0.989	0.997	0.998	0.999	1	1
Chiayi City	0.585	0.846	0.934	0.977	0.989	0.994	0.999	1	1	1
Nantou County	0.606	0.847	0.940	0.976	0.991	0.998	0.999	1	0.999	1
Tainan City	0.587	0.853	0.933	0.968	0.987	0.998	0.999	0.997	1	1
Kaohsiung City	0.609	0.834	0.942	0.977	0.994	0.995	0.998	0.999	0.999	1
Pingtung County	0.635	0.832	0.939	0.978	0.991	0.993	0.998	1	0.999	1
Taitung County	0.595	0.850	0.922	0.965	0.990	0.995	0.999	1	1	1
Hualien County	0.600	0.836	0.945	0.971	0.993	0.998	0.997	1	0.999	1
Yilan County	0.632	0.847	0.939	0.972	0.985	0.996	0.999	0.999	1	1